Supporting Information

Materials and Measurements. Cisplatin was obtained from Strem Chemicals, Inc. Oxaliplatin was purchased from LC Laboratories. All other chemicals and solvents are commercially available. ^{1}H, ^{13}C, and ^{195}Pt NMR spectra were recorded on a Bruker AVANCE-400 or a Varian 500 Spectrometer NMR spectrometer in the Massachusetts Institute of Technology Department of Chemistry Instrumentation Facility (MIT DCIF). Chemical shifts were referenced externally to K_2PtCl_4 in D_2O (δ -1628 ppm) for ^{195}Pt NMR spectra or internally to residual solvent peaks for ^{1}H and ^{13}C NMR spectra. ESI-MS spectra were obtained on an Agilent Technologies 1100 Series LC/MS instrument. Atomic absorption spectroscopic measurements were taken on a Perkin Elmer AAnalyst 600 spectrometer. Distilled water was purified by passage through a Millipore Milli-Q Biocel water purification system (18.2 MΩ) with a 0.22 μm filter. Elemental analyses were performed by a commercial analytical chemistry laboratory. UV-Vis spectroscopy was performed using a HP 8453 UV-visible spectrometer. Emission spectra were obtained by using a QuantaMaster 4 Photon Technology International fluorimeter (Birmingham, NJ) at room temperature. A BioTek Synergy HT multi-detection microplate plate reader was used for MTT assays. GLuc activity was monitored using a luminescence plate reader (Synergy 2, BioTek, Winooski, VT, USA).

General Method to Prepare *cis*-[Pt(NH$_3$)$_2$(Am)Cl]NO$_3$. Nitrate salts of the monofunctional Pt complexes were prepared via a modification of a reported method (Hollis LS, Amundsen AR, Stern EW (1989) *J Med Chem* 32, 128-136), as follows. To a solution of cisplatin (0.3 g, 10 mmol) in 15 mL DMF was added $AgNO_3$ (0.168 g, 1 equiv), and the reaction was stirred under protection from light at 55 °C. After 16 h, the AgCl precipitate was filtered. To the supernatant, Am (*N*-heterocyclic ligands, 0.9 equiv) was added, and the reaction was stirred for 16 h at 55 °C. The reaction mixture was evapo-

rated under reduced pressure and the residue was dissolved in 30 mL of MeOH. Unreacted yellow cisplatin (~10%) was removed by filtration. The filtrate was stirred vigorously, and diethylether (100 ml) was then added to precipitate the desired compound as a solid. The compound was filtered and washed twice with 50 mL of diethylether. The compound was purified by redissolving in methanol and precipitating by adding it dropwise to vigorously stirred diethyl ether. The final compound was isolated by vacuum filtration and dried in vacuo.

***cis*-[Pt(NH$_3$)$_2$(pyridine)Cl]NO$_3$ (pyriplatin).** White solid. Yield: 72%. ESI-MS m/z calculated (M^+): 343.03, found: 343.6. ^{1}H NMR (400 MHz, DMSO-d$_6$): δ 4.30 (3H, broad), 4.64 (3H, broad), 7.57 (2H, t), 8.04 (1H, t), 8.72 (2H, d). ^{13}C NMR (100 MHz, D$_2$O/MeOD): δ 127.7, 140.8, 153.7. ^{195}Pt NMR (86 MHz, D$_2$O): δ -2306. Anal. Calcd. for $C_5H_{11}ClN_4O_3Pt$: C, 14.80; H, 2.73; N, 13.81; Found: C, 15.11; H, 2.83; N, 13.35.

***cis*-[Pt(NH$_3$)$_2$(2-methylpyridine)Cl]NO$_3$.** White solid. Yield: 83%. ESI-MS m/z calculated (M^+): 357.04, found: 357.0. ^{1}H NMR (400 MHz, DMSO-d$_6$): δ 3.00 (3H, s), 4.24 (3H, broad), 4.45 (3H, broad), 7.37 (1H, d), 7.53 (1H, t), 7.86 (1H, t), 8.76 (1H, d). ^{13}C NMR (100 MHz, DMSO-d$_6$): δ 25.7, 123.2, 126.7, 138.7, 153.3, 161.0. ^{195}Pt NMR (86 MHz, DMSO-d$_6$): δ -2298. Anal. Calcd. for $C_6H_{13}ClN_4O_3Pt$: C, 17.17; H, 3.12; N, 13.35; Found: C, 17.22; H, 3.06; N, 13.23.

***cis*-[Pt(NH$_3$)$_2$(2-amino-3-methylpyridine)Cl]NO$_3$.** Brown solid. Yield: 46%. ESI-MS m/z calculated (M^+): 372.06, found: 372.7. ^{1}H NMR (400 MHz, DMSO-d$_6$): δ 2.07 (3H, s), 4.22 (3H, broad), 4.44 (3H, broad), 6.55 (1H, m), 6.94 (1H, s), 7.40 (1H, s), 7.96 (NH, 2H). ^{13}C NMR (100 MHz, DMSO-d$_6$): δ 17.3, 113.1, 138.1, 146.7, 158.3, 187.0. ^{195}Pt NMR (86 MHz, DMSO-d$_6$): δ -2358. Anal. Calcd. for $C_6H_{14}ClN_5O_3Pt$: C, 16.58; H, 3.25; N, 16.11; Found: C, 16.11; H, 3.41; N, 16.34.

***cis*-[Pt(NH$_3$)$_2$(quinoline)Cl]NO$_3$ (quinoplatin).** White solid. Yield: 70%. ESI-MS m/z calculated (M^+): 394.04, found: 393.9. ^{1}H NMR (400 MHz, DMSO-d$_6$): δ 4.39 (3H, broad), 4.55 (3H, broad), 7.69 (1H, t), 7.79 (1H, t), 8.05 (1H, t), 8.15 (1H, d), 8.68 (1H, d), 9.26 (1H, s), 9.54 (1H, d). ^{13}C NMR (100 MHz, DMSO-d$_6$): δ 122.6, 128.3, 128.2, 128.7, 129.4, 131.3, 139.3, 146.8, 155.9. ^{195}Pt NMR (86 MHz, DMSO-d$_6$): δ -2294. Anal. Calcd. for $C_9H_{13}ClN_4O_3Pt$: C, 23.72; H, 2.88; N, 12.29; Found: C, 24.06; H, 2.88; N, 12.29.

***cis*-[Pt(NH$_3$)$_2$(isoquinoline)Cl]NO$_3$.** White solid. Yield: 74%. ESI-MS m/z calculated (M^+): 394.04, found: 393.9. ^{1}H NMR (400 MHz, DMSO-d$_6$): δ 4.34 (3H, broad), 4.69 (3H, broad), 7.86 (1H, s), 8.00 (2H, m), 8.12 (1H, d), 8.29 (1H, d), 8.55 (1H, d), 9.63 (1H, s). ^{13}C NMR (100 MHz, DMSO-d$_6$): δ 123.0, 126.5, 128.3, 129.2, 130.9, 133.4, 135.1, 136.8, 144.5, 156.8, 163.2. ^{195}Pt NMR (86 MHz, DMSO-d$_6$): δ -2282. Anal. Calcd. for $C_9H_{13}ClN_4O_3Pt$: C, 23.72; H, 2.88; N, 12.29; Found: C, 23.82; H, 2.88; N, 12.20.

***cis*-[Pt(NH$_3$)$_2$(1-methylimidazole)Cl]NO$_3$.** White solid. Yield: 66%. ESI-MS m/z calculated (M^+): 346.04, found: 347.0. ^{1}H NMR (400 MHz, DMSO-d$_6$): 3.73 (3H, s), 4.16 (3H, broad), 4.53 (3H, broad), 7.13 (1H, s), 7.33 (1H, s), 8.14 (1H, s). ^{13}C NMR (100 MHz, DMSO-d$_6$): δ 34.3, 121.5, 128.2, 139.6. ^{195}Pt NMR (86 MHz, DMSO-d$_6$): δ -2316. Anal. Calcd. for $C_4H_{12}ClN_5O_3Pt$: C, 11.76; H, 2.96; N, 17.14; Found: C, 11.91; H, 2.96; N, 17.12.

***cis*-[Pt(NH$_3$)$_2$(acridine)Cl]NO$_3$.** Yellow solid. Yield: 45%. ESI-MS m/z calculated (M^+): 443.06, found: 443.1. ^{1}H NMR (400 MHz, DMSO-d$_6$): 4.52 (6H, broad), 7.79 (2H, t, J = 8 Hz), 8.21 (2H, t, J = 8 Hz), 8.33 (2H, d, J = 8 Hz), 9.55 (1H, s), 10.23 (2H, d, J = 8 Hz). ^{13}C NMR (100 MHz, DMSO-d$_6$): δ 126.9, 127.2, 128.4, 129.1, 132.9, 141.4, 148.8. ^{195}Pt NMR (86 MHz, DMSO-d$_6$): δ -2246. Anal. Calcd. for $C_{13}H_{15}ClN_4O_3Pt$: C, 30.87; H, 2.99; N, 11.08; Found: C, 30.89; H, 3.06; N, 10.98.

***cis*-[Pt(NH_3)$_2$(benzo[f]quinoline)Cl]NO_3.** White solid. Yield: 62%. ESI-MS m/z calculated (M^+): 443.06, found: 442.9. ^{1}H NMR (400 MHz, DMSO-d_6): 4.49 (6H, broad), 7.86 (3H, t, J = 8 Hz), 8.20 (1H, s), 8.43 (1H, d, J = 12 Hz), 8.97 (1H, d, J = 12 Hz), 9.93 (1H, s), 9.56 (2H, t, J = 8 Hz). ^{13}C NMR (100 MHz, DMSO-d_6): δ 78.3, 89.4, 93.5, 124.2, 129.1, 130.9, 132.4, 146.9, 155.1, 160.3. ^{195}Pt NMR (86 MHz, DMSO-d_6): δ -2284. Anal. Calcd. for $C_{13}H_{15}ClN_4O_3Pt$: C, 30.87; H, 2.99; N, 11.08; Found: C, 30.91; H, 2.91; N, 10.83.

X-Ray Crystal Structure Refinement Details.

The nitrate counterion of quinoplatin was disordered over two orientations. This disorder was modeled with similarity restraints, and the occupancy factor refined to 0.65 for the major component. A solvent accessible void of 65 Å^3 also remained in the crystal lattice around the crystallographic inversion center. The highest residual electron density in the structure (2.9 e^-) occupies this void at the inversion center. Attempts to model the residual density as a disordered molecule of methanol were unsuccessful. After complete refinement of the structure, visualization of the anisotropic displacement parameters of the quinoline ring revealed elongated and abnormally shaped ellipsoids. These features are tentatively attributed a small degree of whole molecule disorder, which was not modeled.

The refinement of phenanthriplatin proceeded normally. At the end of refinement, however, a large residual electron density peak of 3.524 e/Å^3 remained. This peak is located 0.91 Å from the platinum center and may be due to an imperfect absorption correction.

Cell Lines and Cell Culture. Human colon carcinoma HT29, human breast carcinoma MCF7, human bone sarcoma U2OS, human prostate carcinoma PC3, human testis carcinoma NTera2, and human cervix carcinoma HeLa cells were obtained from the American Type Culture Collection (ATCC). Human lung carcinoma cell lines A549 and normal lung fibroblast MRC5 were provided by David E. Root

(Whitehead Institute for Biomedical Research). Cells were incubated at 37 °C in 5% CO_2 and grown in RPMI (HT29 and PC3) or DMEM (A549, MRC5, HeLa, MCF7, Ntera2, and U2OS) supplemented with 10% fetal bovine serum and 1% penicillin/streptomycin. Cells were passed every 3 to 4 days and restarted from a frozen stock upon reaching passage number 20.

MTT Assay. The cytotoxicities of cisplatin, oxaliplatin, and monofunctional Pt(II) compounds were evaluated by the MTT assay. Solutions of the platinum compounds were freshly prepared in sterile PBS before use and their concentrations quantitated by atomic absorption spectroscopy. Cells were seeded in a 96-well plate (1200 cells per well for cancer cells and 1800 cells per well for the normal lung fibroblasts) in 100 µL of RPMI or DMEM and incubated for 24 h. The cells were then treated with cisplatin, oxaliplatin, or a monofunctional Pt(II) complex, separately at varying concentrations, for an incubation period of 72 h at 37 °C. The cells were then treated with 20 µL of 3-(4,5-dimethylthiazol-2-yl)-2,5-diphenyltetrazolium bromide (MTT) (5 mg/mL in PBS) and incubated for 4 h. The medium was removed, 100 µL of DMSO was added to the cells, and the absorbance of the purple formazan dye was recorded at 560 nm using a BioTek Synergy HT multi-detection microplate plate reader. For each cell line, three independent experiments were carried out in triplicate.

Cellular Uptake of Platinum. Approximately 10^6 cells were seeded in a 60 mm diameter Petri dish in triplicate in the culture medium and were incubated overnight to attach. For platinum accumulation, the cells were treated with 5 µM of cisplatin, pyriplatin, or phenanthriplatin at 37 °C in 5% CO_2 for 3 h. After incubation, the medium was removed and cells were washed with 2 mL of ice-cold PBS three times to remove excess Pt. The cells were detached using 1 mL trypsin, and then transferred to a centrifuge tube using an additional 0.5 mL PBS. The cells were pelleted by centrifugation at 200 x *g* and 4 °C for 20 min. The cell pellets obtained were resuspended in 200 µL of ice-cold lysis buffer (1.0 mM dithiothreitol (DTT), 1.0 mM phenylmethanesulfonylfluoride (PMSF), 10 mM KCl, and 10 mM

$MgCl_2$, pH 7.5) and then cooled for 15 min in an ice bath. The cells were centrifuged at 450 x *g* and 4 °C for 20 min. After removing the supernatant, the pellets were resuspended in 150 µL of ice-cold lysis buffer for the cytoplasm and nuclear fraction isolations. The cell membranes were lysed using 10 strokes of a 28-gauge syringe. The resultant suspension was centrifuged at 11,000 x *g* for 20 min at 4 °C, and the supernatant was retained as the cytosolic fraction. The nuclear pellet was resuspended in 150 µL of extraction buffer (1.0 mM DTT, 1.0 mM PMSF, 1.5 mM $MgCl_2$, 0.2 M ethylenediaminetetraacetic acid (EDTA), 0.42 M NaCl, and 25% glycerol, pH 7.9) and lysed by 10 strokes of a 28-gauge syringe. The lysate was shaken at 1,000 rpm for 1 h at 4 °C and centrifuged at 20,000 x *g* for 10 min at 4 °C. The nuclear fraction was collected as supernatant. To evaluate whole cell uptake, 150 µL of concentrated nitric acid was added to washed cell pellets, and cells were digested for 2 h at 90 °C. Platinum concentrations in all of the fractions were determined by AAS.

Fluorescence Scatchard Plots. Calf-thymus DNA was purchased from Invitrogen. Ethidium bromide was obtained from Sigma-Aldrich. For all fluorescence measurements, the excitation wavelength was 525 nm, and the emission was monitored between 560 and 640 nm. The buffer used in the fluorescent Scatchard plot studies was 50 mM Tris-HCl and 0.2 M NaCl, pH 7.5. Cisplatin, pyriplatin, phenanthriplatin, or [Pt(terpy)Cl]Cl (r_f = 0 ~ 2) was incubated with 10.8 µM of calf-thymus DNA for 1 min or 12.1 µM for 12 h at room temperature before adding ethidium bromide. The ethidium bromide concentration varied from 2.2 to 23.5 µM.

A plot of r/c_f versus r is described by $r/c_f = K(n-r)$, where c_f is the concentration of unbound ethidium bromide and r is the ratio of bound ethidium bromide to total nucleotide concentration [DNA]. The plot therefore provides the intrinsic binding constant (K) for ethidium bromide (slope) and the maximum value of r (n, the intercept of the abscissa).

Preparation of Globally Platinated Plasmids. A 125 μg/mL (46 nM) portion of pGLuc plasmid dissolved in 24 mM Na-HEPES pH 7.4 and 10 mM NaCl buffer was treated with cisplatin (0, 2.95, 5.73, 11.35, 22.43 μM), pyriplatin (0, 6.53, 15.98, 30.49, 59.32 μM), or phenanthriplatin (0, 3.18, 7.56, 11.78, 23.82 μM) for 16 h at 37 °C. The resulting mixtures were dialyzed (molecular weight cut-off 3.5 kDa) against ddH_2O overnight at 4 °C with five changes of ddH_2O. The r_b values (bound Pt/nucleotide) were determined by UV/Vis and atomic absorption spectroscopy. A series of plasmids with Pt/plasmid ratios ranging from 0 to ~ 120 was prepared by reaction with cisplatin, pyriplatin, or phenanthriplatin. The level of DNA-bound pyriplatin or phenanthriplatin per amount added was almost identical to that of cisplatin, as revealed by plots of r_b vs. r_f (Fig. S10).

Transient Transfection of Cells for Transcription Assays. A549 cells were plated in 96-well plates at 2,000 cells/well and HT29 cells were plated in 96-well plates at 6,000 cells/well. After 48 h incubation (allowing cells to achieve ~ 30% confluence), cells were transfected with 50 ng of platinated plasmid in 25 μL Opti-MEM and 0.125 μL Lipofectamine 2000, and subsequently 50 μL of antibiotics-free DMEM supplemented with 10% FBS. After 2 h, the cells were washed with medium and 100 μL of fresh medium was added. The experiment was carried out in quadruplicate.

GLuc Luminometry Assay. A 10 μL volume of medium at different time points (12, 24, 36, 48, 60 h) was transferred into opaque white 96-well plates, and 25 μL of GLuc assay solution (10 μM coelenterazine (NanoLight Technologies, Pinetop, AZ, USA) in 2.5 mM acidified methanol (100 mM HCl), buffer (10 mM Tris-HCl pH 7.8, 1 mM EDTA, 0.6 M NaCl) was added by the automatic injector of the instrument.

Table S1. X-Ray crystallographic data collection and refinement parameters

	quinoplatin	**phenanthriplatin**
formula	$C_9H_{13}ClN_4O_3Pt$	$C_{13}H_{15}ClN_4O_3Pt$
fw	455.77	505.83
space group	$P2_1/c$	*Pbca*
a, Å	13.7876(12)	11.946(2)
b, Å	7.9528(7)	10.3474(18)
c, Å	13.1785(11)	24.754(4)
β, deg	104.7600(10)	
V, Å^3	1397.3(2)	3059.7(9)
Z	4	8
ρ_{calcd}, g·cm^{-3}	2.166	2.196
T, °C	-173(2)	-173(2)
μ(Mo Kα), mm^{-1}	10.238	9.364
Θ range, deg	3.02 to 29.57	1.65 to 25.13
total no. of data	28531	43571
no. of unique data	3908	2724
no. of restraints	76	0
no. of parameters	193	201
completeness to Θ (%)	99.7	99.8
R1[a] (%)	4.20	4.52
wR2[b] (%)	9.97	9.18
GOF[c]	1.077	1.116
max, min peaks, e·Å^{-3}	2.915, -1.675	3.524, -1.089

[a] $R1 = \Sigma||F_o| - |F_{cll}/\Sigma|F_o|$. [b] $wR2 = \{\Sigma[w(F_o^2 - F_c^2)^2]/\Sigma[w(F_o^2)^2]\}^{1/2}$. [c] $GOF = \{\Sigma[w(F_o^2 - F_c^2)^2]/(n - p)\}^{1/2}$ where *n* is the number of data and *p* is the number of refined parameters.

Table S2. Selected interatomic distances (Å) and angles (deg) for quinoplatin and phenanthriplatin [a]

	quinoplatin	phenanthriplatin
Pt(1) –N(1)	2.038(6)	2.036(6)
Pt(1) –N(2)	2.037(6)	2.040(6)
Pt(1) –N(3)	2.036(6)	2.032(6)
Pt(1) –Cl(1)	2.3009(16)	2.2998(19)
N(1) –Pt(1) –N(2)	88.9(2)	89.4(3)
N(1) –Pt(1) –N(3)	179.2(2)	176.4(2)
N(1) –Pt(1) –Cl(1)	89.41(18)	90.51(19)
N(2) –Pt(1) –N(3)	90.3(2)	94.2(3)
N(2) –Pt(1) –Cl(1)	177.91(17)	178.26(19)
N(3) –Pt(1) –Cl(1)	91.35(15)	85.90(18)

[a] Atoms are labeled as indicated in Figures S1 and S2. The numbers in the parentheses are the estimated standard deviations of the last significant figures.

Table S3. IC_{50} values* for cisplatin and monofunctional Pt(II) compounds in the various cell lines for a 72-h incubation period

IC_{50} (μM)	**A549**	**MRC5**	**HT29**	**HeLa**	**U2OS**
cisplatin	6.75 ± 0.38	6.18 ± 0.16	15.9 ± 1.5	1.77 ± 0.72	7.15 ± 0.25
***cis*-[Pt(NH_3)$_2$(pyridine)Cl]NO_3**	52.1 ± 2.3	92.1 ± 9.9	144 ± 10	31.3 ± 2.8	78.9 ± 6.7
***cis*-[Pt(NH_3)$_2$ (2-methylpyridine)Cl]NO_3**	50.6 ± 1.7	58.9 ± 4.2	63.8 ± 1.9	not measured	not measured
***cis*-[Pt(NH_3)$_2$ (2-amino-3-methylpyridine)-Cl]NO_3**	47.1 ± 1.4	51.7 ± 7.7	72.9 ± 4.6	not measured	not measured
***cis*-[Pt(NH_3)$_2$(quinoline)Cl]NO_3**	8.11 ± 0.68	23.5 ± 1.6	38.0 ± 4.5	12.2 ± 0.8	23.5 ± 2.7
***cis*-[Pt(NH_3)$_2$(isoquinoline)Cl]NO_3**	11.5 ± 0.4	26.4 ± 1.0	45. 6 ± 2.7	not measured	not measured
***cis*-[Pt(NH_3)$_2$ (1-methylimidazole)-Cl]NO_3**	62.0 ± 0.8	40.5 ± 1.1	53.4 ± 8.5	not measured	not measured
***cis*-[Pt(NH_3)$_2$(acridine)Cl]NO_3**	3.74 ± 0.01	9.17 ± 0.47	13.5 ± 0.7	2.69 ± 0.10	4.42 ± 0.31
***cis*-[Pt(NH_3)$_2$(benzo[f]quinoline)Cl]NO_3**	0.83 ± 0.03	not measured	not measured	0.64 ± 0.01	0.88 ± 0.01
***cis*-[Pt(NH_3)$_2$(phenanthridine)-Cl]NO_3**	0.22 ± 0.01	0.86 ± 0.06	2.02 ± 0.04	0.30 ± 0.02	0.59 ± 0.04

*Data reflect the mean and standard deviation of results from three separate experiments, each performed in triplicate.

Figure Legends

Fig. S1. Thermal ellipsoid plot of the X-ray crystal structure of quinoplatin. Ellipsoids are drawn at the 50% probability level. The nitrate anion is not shown.

Fig. S2. Thermal ellipsoid plot of the X-ray crystal structure of phenanthriplatin. Ellipsoids are drawn at the 50% probability level. The nitrate anion is not shown.

Fig. S3. Comparative analysis of cytotoxicity of anticancer agents in the NCI-60 tumor cell line panel. The indicated values are calculated as follows: log[(GI50 individual cell line)-mean (logGI50)]. Negative values indicate that the cell line is more sensitive than the average, whereas positive values indicate that the cell line is more resistant than the average. The abscissae are presented on a log scale. Data of cisplatin and oxaliplatin are obtained from the NCI web site at http://dtp.nci.nih.gov/webdata.html.

Fig. S4. ^{1}H NMR spectral study of the aquation of monofunctional Pt(II) complexes, (A) pyriplatin and (B) phenanthriplatin, at 37 ^{o}C in D_2O over time. The red box denotes the peaks that were integrated for analysis.

Fig. S5. Progression of pyriplatin and phenanthriplatin aquation in D_2O at 37 °C, as monitored by ^{1}H NMR spectroscopy over time.

Fig. S6. 1-D ^{1}H NMR spectra of the reaction between monofunctional Pt(II) complexes and 5'-dGMP under pseudo-first order conditions at 37 ^{o}C in 10 mM PBS, pH* 7.4. The reaction time is given for each spectrum on the left and the resonance assignment was labeled for each aromatic proton on the ligand. The arrow points to the peak chosen to be integrated for computing the concentrations of the platinum complex. (A) pyriplatin and (B) phenanthriplatin.

Fig. S7. Pseudo-first-order treatment of the kinetic data of pyriplatin and phenanthriplatin with excess 5'-dGMP (1:16, 2 mM:32 mM) at 37 °C in 10 mM PBS. The calculated rate constants (*k*, 37 ^{o}C) for

phenanthriplatin and pyriplatin are 0.29 ± 0.05 h^{-1} and 0.22 ± 0.02 h^{-1} respectively. The calculated half-lives are 3.2 ± 0.3 h and 2.4 ± 0.4 h for phenanthriplatin and pyriplatin, respectively.

Fig. S8. 1-D ^{1}H NMR spectra of the reaction between monofunctional Pt(II) complexes and *N*-AcMet at a 1:1 ratio (2 mM each) at 37 ^{o}C in 10 mM PBS, pH* 7.4. The reaction time is given for each spectrum on the left and the resonance assignment was labeled for each aromatic proton on the ligand. The arrow points to the peak chosen to be integrated for calculation of the concentrations of platinum complex. (A) pyriplatin and (B) phenanthriplatin.

Fig. S9. Second order treatment of the kinetic data of pyriplatin and phenanthriplatin with an equal concentration of *N*-AcMet (2 mM) at 37 °C in 10 mM PBS. The calculated rate constants (*k*, 37 ^{o}C) for phenanthriplatin and pyriplatin are 0.034 ± 0.005 $mM^{-1}h^{-1}$ and 0.56 ± 0.30 $mM^{-1}h^{-1}$ respectively. The estimated half-lives are 15.0 ± 2.4 h and 1.04 ± 0.56 h respectively.

Fig. S10. Characterization of the reaction products of (A) pyriplatin and (B) phenanthriplatin with *N*-AcMet after 48 hours in D_2O, 10 mM PBS, pH* 7.4, by ESI-MS (methanol with 0.1% of formic acid). In panel A, product **1** may arise from displacement of a chloride ligand by *N*-AcMet, followed by release of ammonia and binding of chloride from the buffer owing to the strong kinetic trans effect of the sulfur donor. Product **2** may form by replacement of chloride by formate ion introduced in preparing a sample for the ESI-MS measurement. In panel B, the starting phenanthriplatin **1** still remains owing to its slower reaction rate, and the *N*-AcMet analogue of **2** in panel (A) is also clearly present. The formate derivative is absent, again most likely a result of the more kinetically inert character of phenanthriplatin compared to pyriplatin.

Fig. S11. Fluorescence Scatchard plots of the binding of ethidium bromide to calf-thymus DNA after 1 min incubation (A) and 12 h incubation (b) in solution of various Pt(II) complexes with varying r_f values.

Fig. S12. Transcription profiles of globally platinated probes in A549 (upper) and HT29 (lower) cells.

Fig. S13. Platination of pGLuc after treatment with cisplatin, pyriplatin, or phenanthriplatin for 16 h at 37 °C in buffer (24 mM HEPES pH 7.4, 10 mM NaCl).

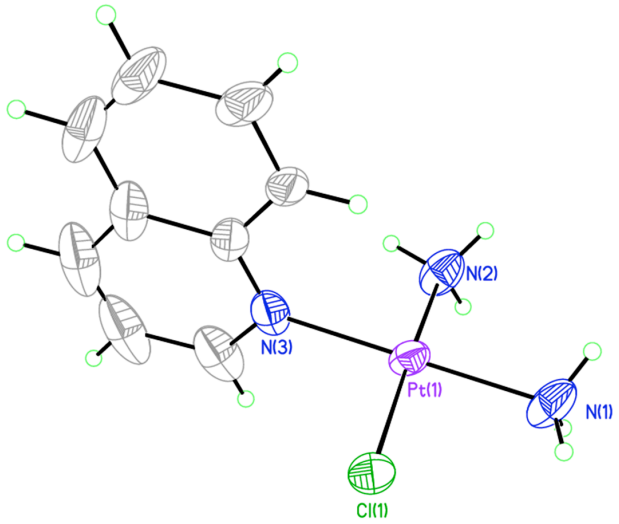

Fig. S1.

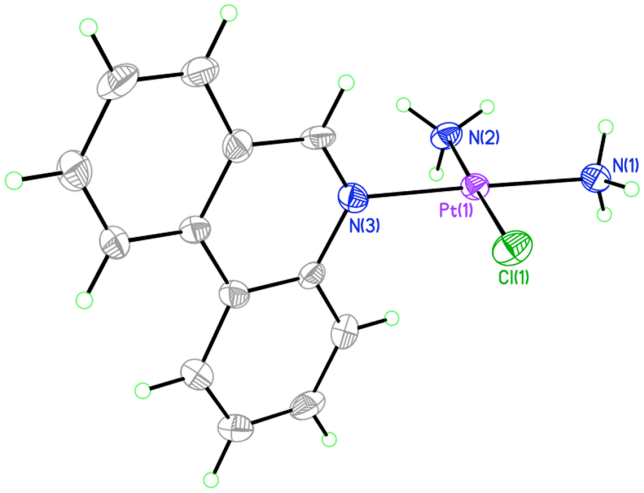

Fig. S2.

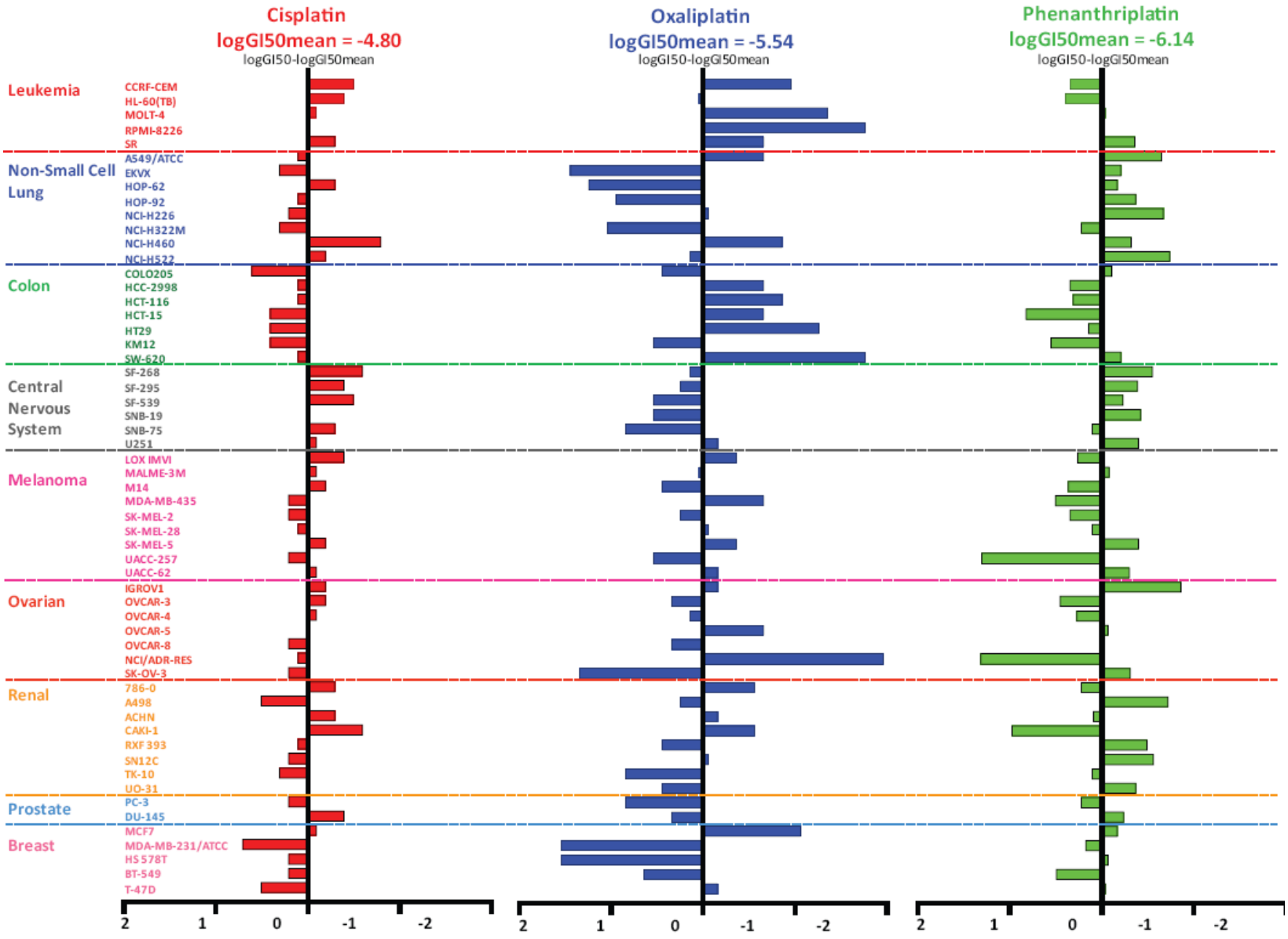
Cisplatin
logGI50mean = -4.80
logGI50-logGI50mean
Oxaliplatin
logGI50mean = -5.54
logGI50-logGI50mean
Phenanthriplatin
logGI50mean = -6.14
logGI50-logGI50mean
Leukemia
CCRF-CEM
HL-60(TB)
MOLT-4
RPMI-8226
SR
Non-Small Cell Lung
A549/ATCC
EKVX
HOP-62
HOP-92
NCI-H226
NCI-H322M
NCI-H460
NCI-H522
Colon
COLO205
HCC-2998
HCT-116
HCT-15
HT29
KM12
SW-620
Central Nervous System
SF-268
SF-295
SF-539
SNB-19
SNB-75
U251
Melanoma
LOX IMVI
MALME-3M
M14
MDA-MB-435
SK-MEL-2
SK-MEL-28
SK-MEL-5
UACC-257
UACC-62
Ovarian
IGROV1
OVCAR-3
OVCAR-4
OVCAR-5
OVCAR-8
NCI/ADR-RES
SK-OV-3
Renal
786-0
A498
ACHN
CAKI-1
RXF 393
SN12C
TK-10
UO-31
Prostate
PC-3
DU-145
Breast
MCF7
MDA-MB-231/ATCC
HS 578T
BT-549
T-47D
2
1
0
-1
-2

Fig. S3.

A.

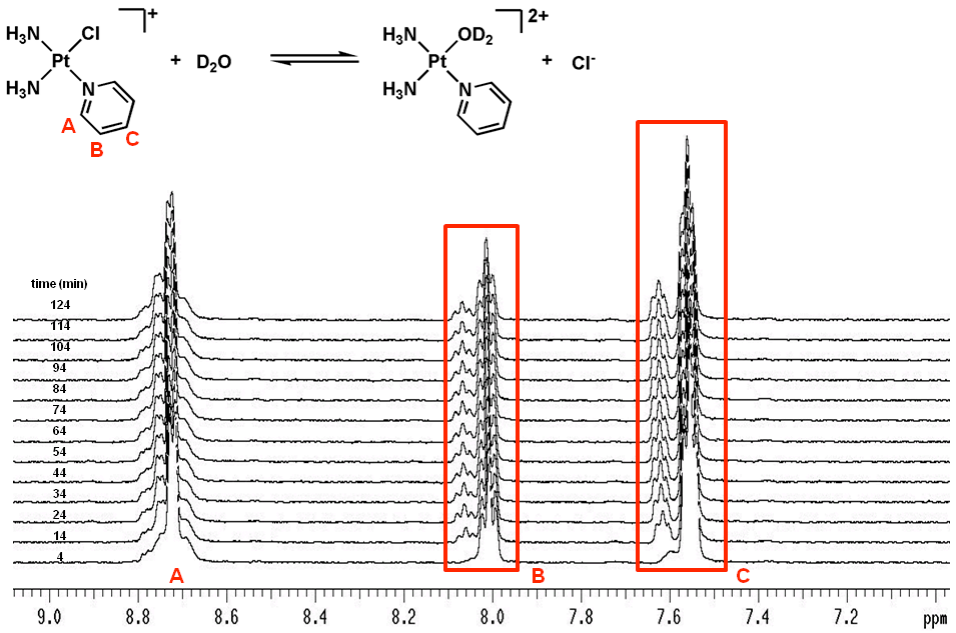
H3N
Cl
Pt
H3N
N
+
D2O
OD2
2+
Cl-
A
B
C
time (min)
124
114
104
94
84
74
64
54
44
34
24
14
4
9.0
8.8
8.6
8.4
8.2
8.0
7.8
7.6
7.4
7.2
ppm

B.

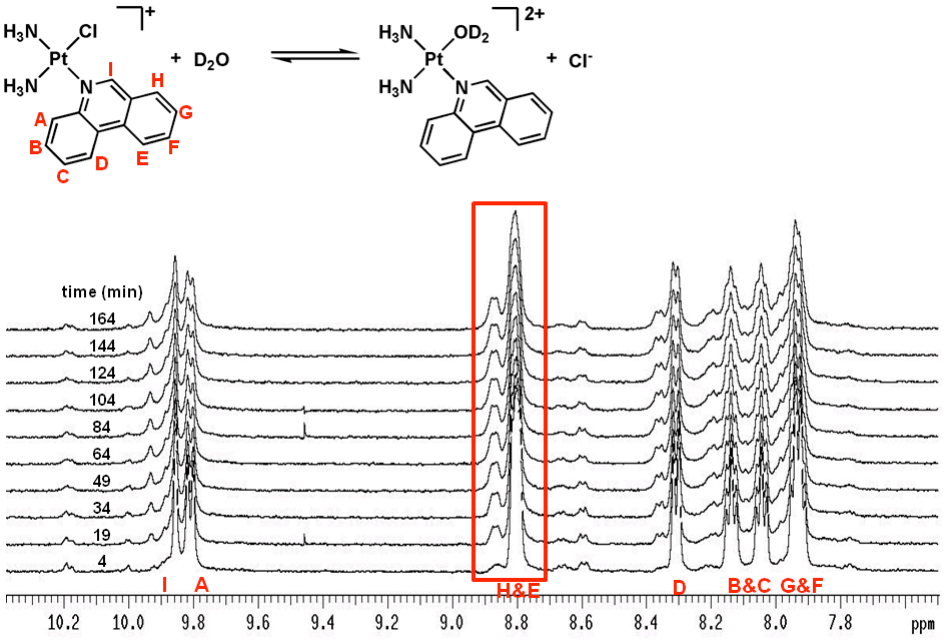
H3N
Cl
Pt
H3N
N
+
D2O
OD2
2+
Cl-
I
H
G
A
B
C
D
E
F
time (min)
164
144
124
104
84
64
49
34
19
4
I
A
H&E
D
B&C
G&F
10.2
10.0
9.8
9.6
9.4
9.2
9.0
8.8
8.6
8.4
8.2
8.0
7.8
ppm

Fig. S4.

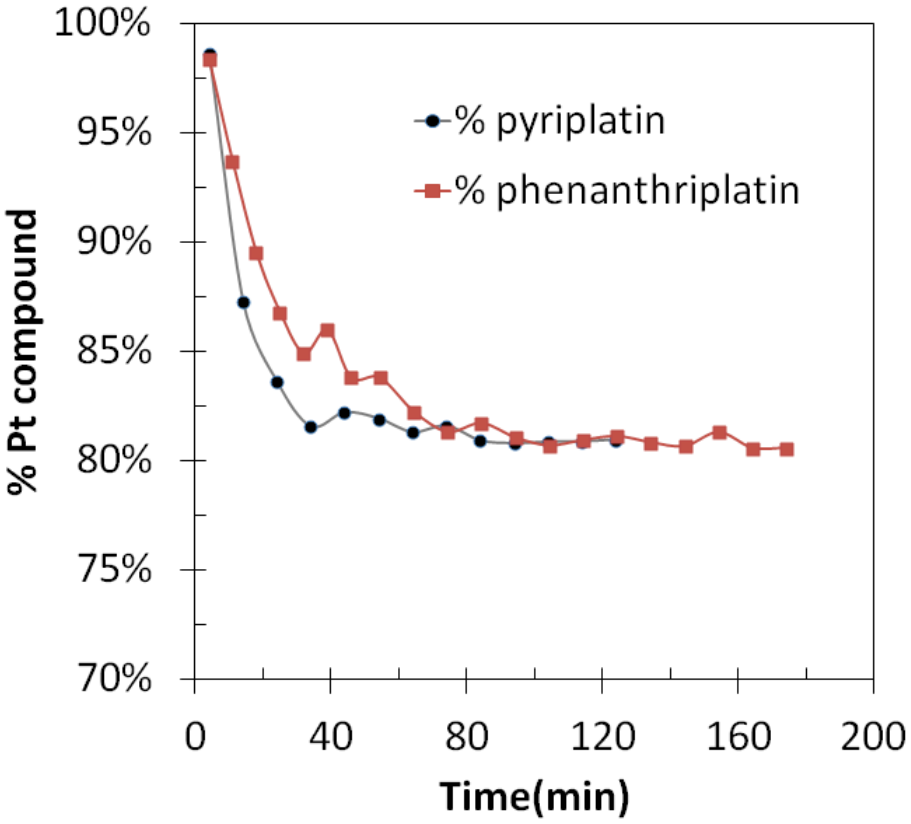
100%
95%
90%
85%
80%
75%
70%
% Pt compound
% pyriplatin
% phenanthriplatin
0
40
80
120
160
200
Time(min)

Fig. S5.

A.

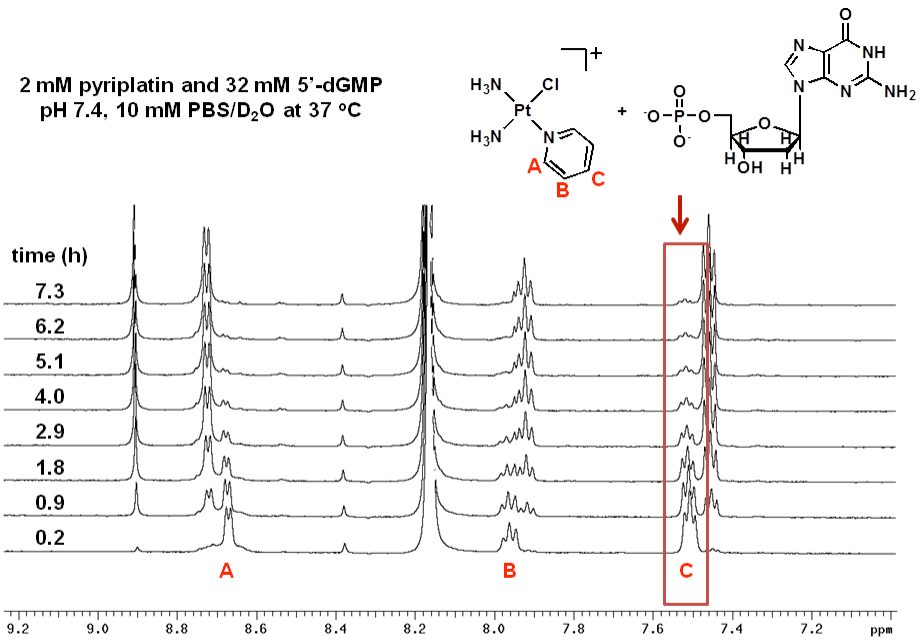
2 mM pyriplatin and 32 mM 5'-dGMP
pH 7.4, 10 mM PBS/D2O at 37 °C
time (h)
7.3
6.2
5.1
4.0
2.9
1.8
0.9
0.2
A
B
C
ppm

B.

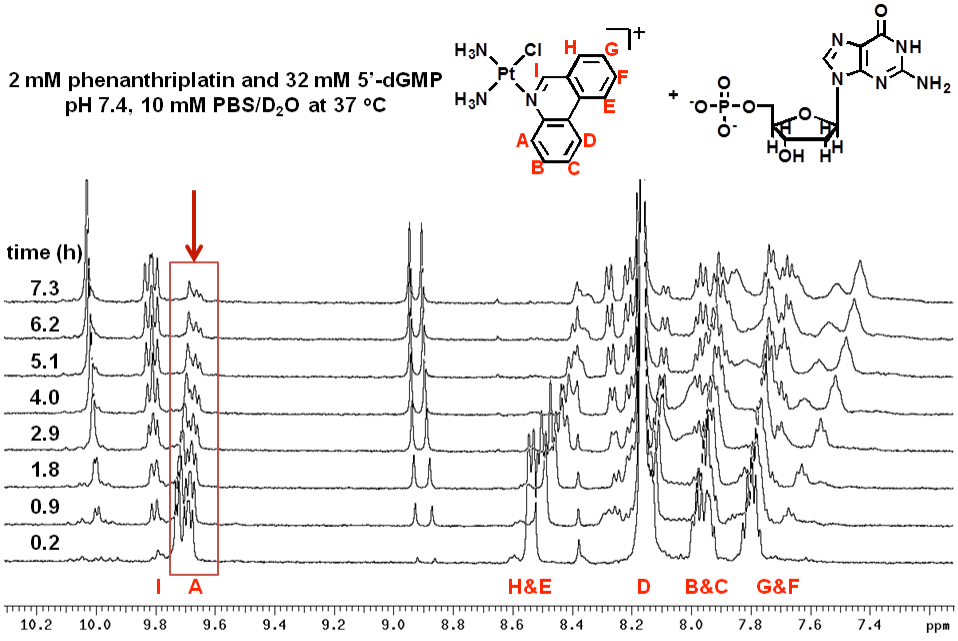
2 mM phenanthriplatin and 32 mM 5'-dGMP
pH 7.4, 10 mM PBS/D2O at 37 °C
time (h)
7.3
6.2
5.1
4.0
2.9
1.8
0.9
0.2
I
A
H&E
D
B&C
G&F
ppm

Fig. S6.

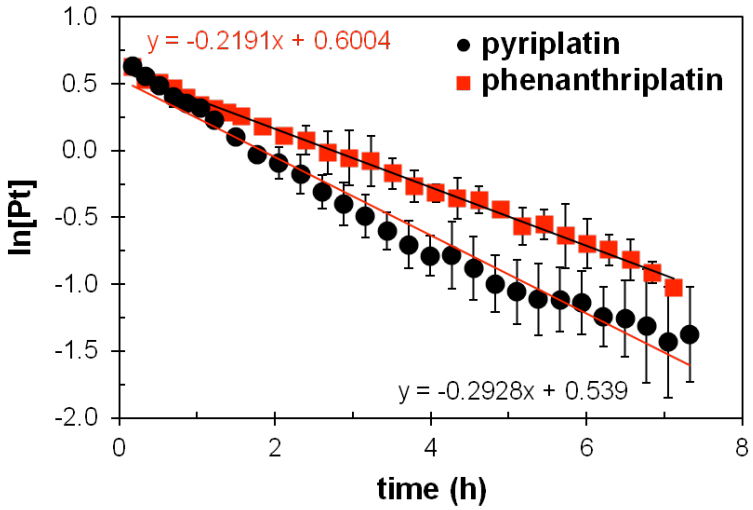
y = -0.2191x + 0.6004
pyriplatin
phenanthriplatin
y = -0.2928x + 0.539
ln[Pt]
time (h)
1.0
0.5
0.0
-0.5
-1.0
-1.5
-2.0
0
2
4
6
8

Fig. S7.

A.

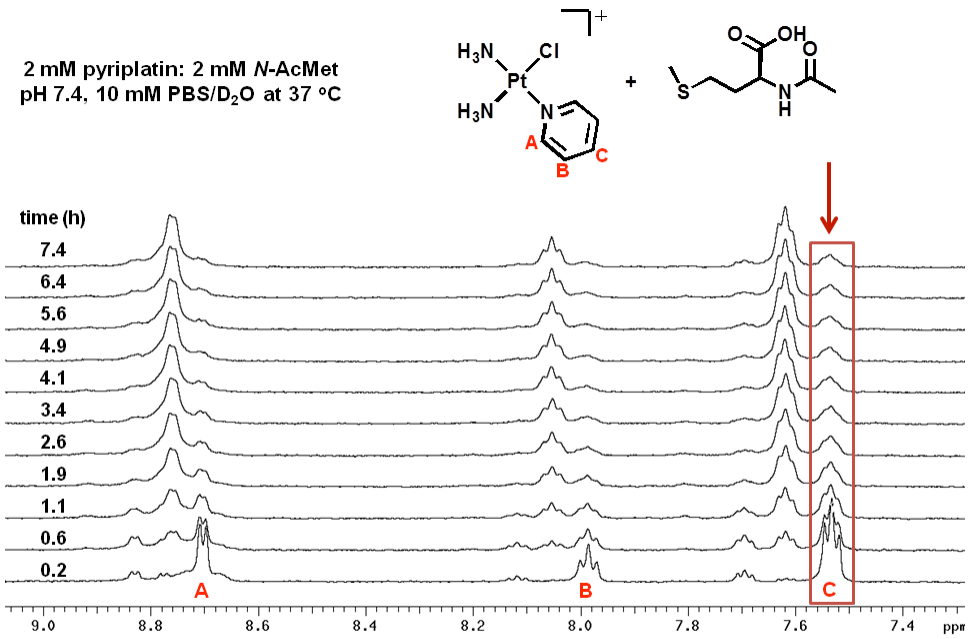
2 mM pyriplatin: 2 mM N-AcMet
pH 7.4, 10 mM PBS/D2O at 37 °C
time (h)
7.4
6.4
5.6
4.9
4.1
3.4
2.6
1.9
1.1
0.6
0.2
A
B
C
9.0
8.8
8.6
8.4
8.2
8.0
7.8
7.6
7.4
ppm

B.

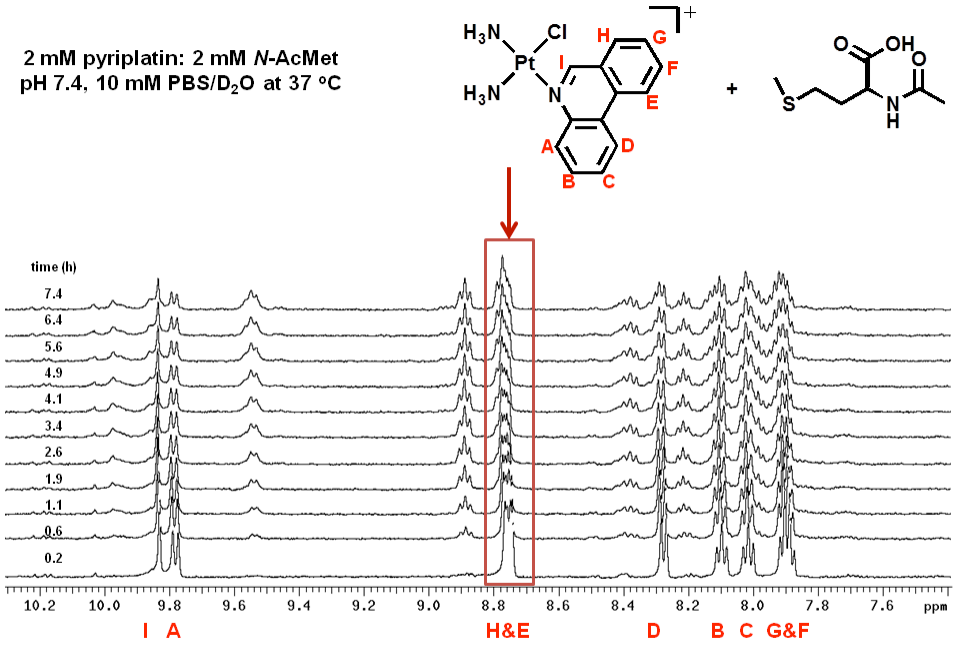
2 mM pyriplatin: 2 mM N-AcMet
pH 7.4, 10 mM PBS/D2O at 37 °C
time (h)
7.4
6.4
5.6
4.9
4.1
3.4
2.6
1.9
1.1
0.6
0.2
10.2
10.0
9.8
9.6
9.4
9.2
9.0
8.8
8.6
8.4
8.2
8.0
7.8
7.6
ppm
I A
H&E
D
B C G&F

Fig. S8.

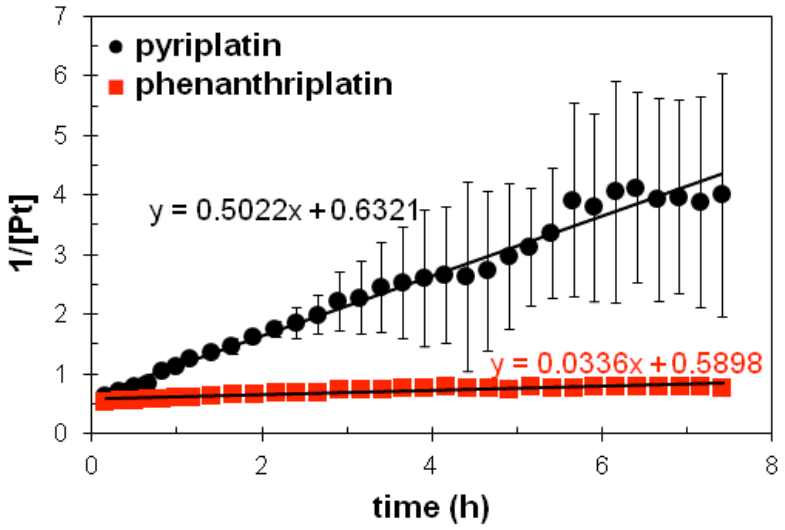

Fig. S9.

A.

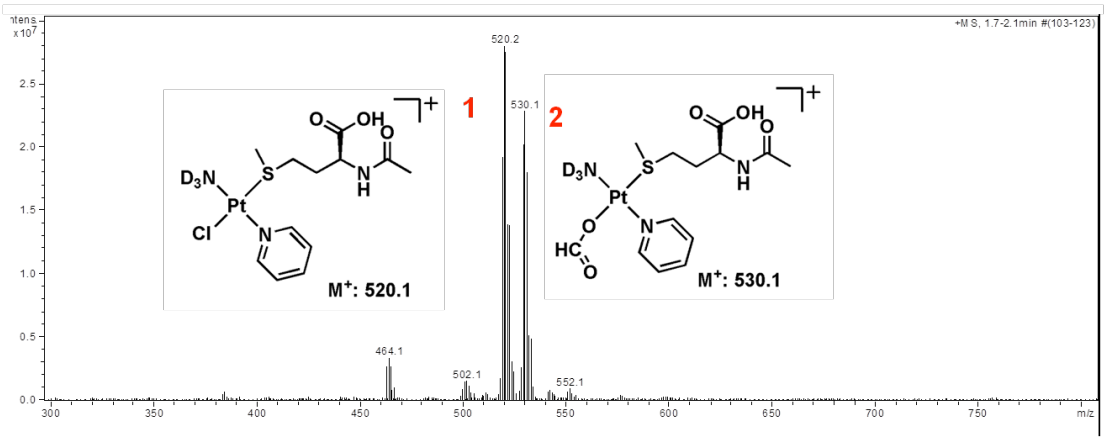

B.

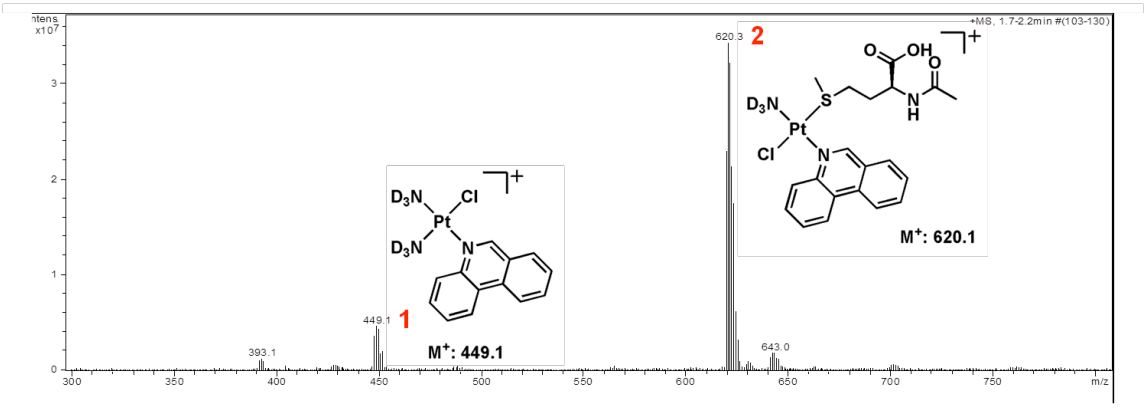

Fig. S10.

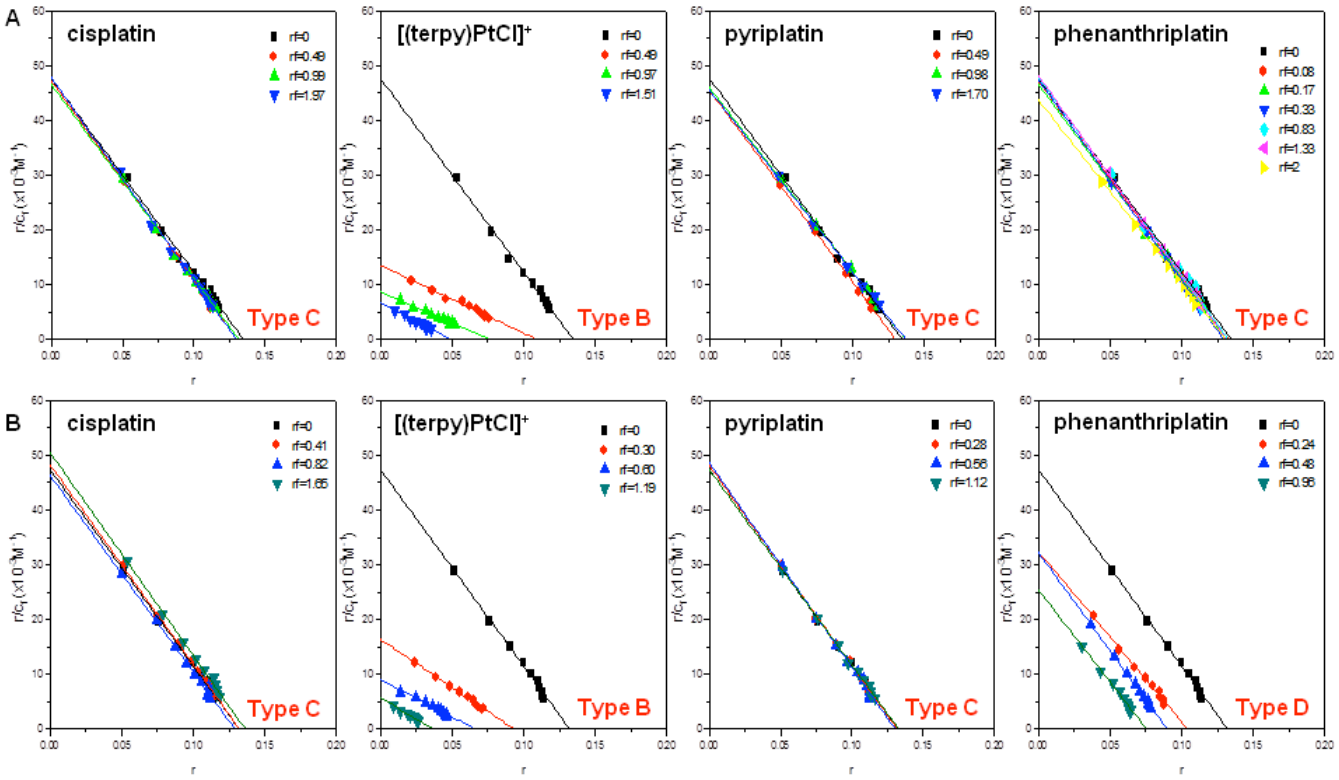

Fig. S11.

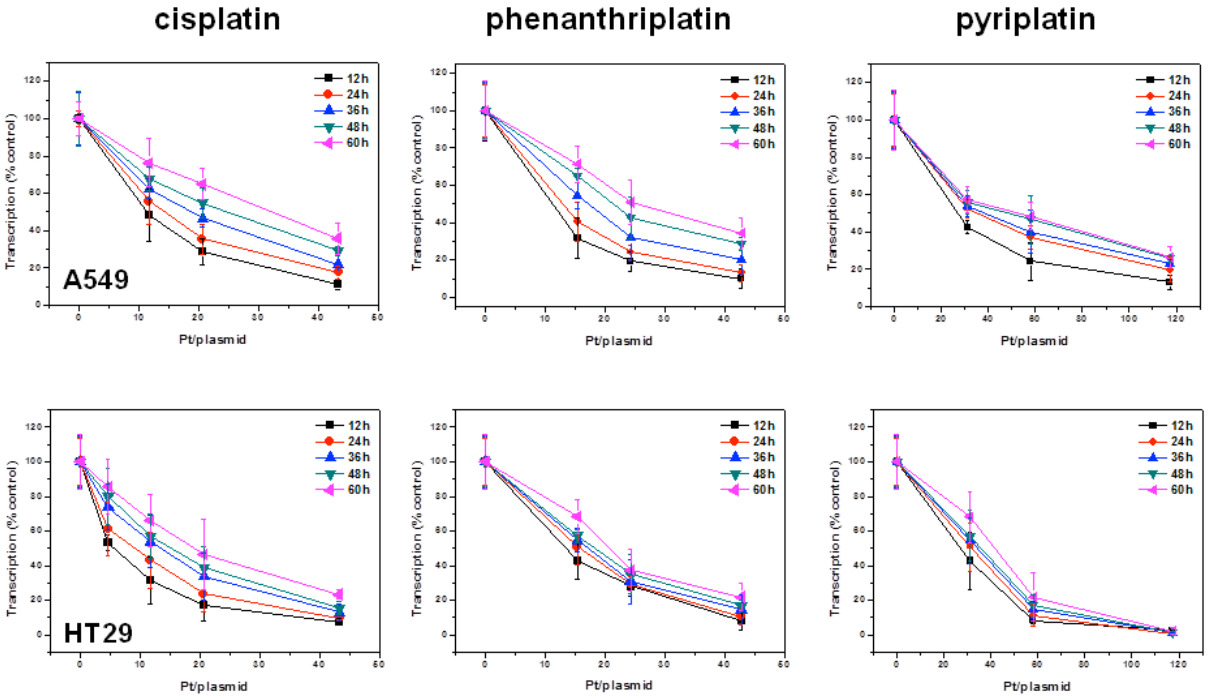

Fig. S12.

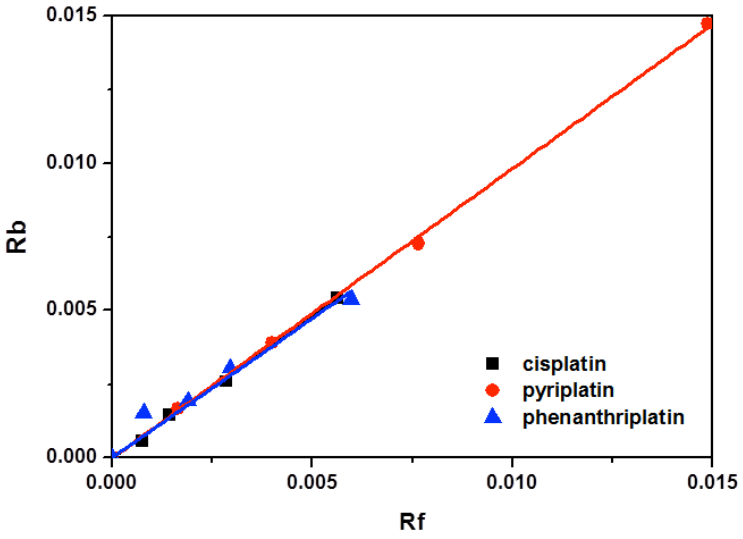
0.015
0.010
0.005
0.000
Rb
0.000
0.005
0.010
0.015
Rf
cisplatin
pyriplatin
phenanthriplatin

Fig. S13.